

Energetic and financial evaluation of solar assisted heat pump space heating systems



Evangelos Bellos*, Christos Tzivanidis, Konstantinos Moschos, Kimon A. Antonopoulos

National Technical University of Athens, School of Mechanical Engineering, Thermal Department, Heroon Polytechniou 9, 157 73 Zografou, Athens, Greece

ARTICLE INFO

Article history:

Received 15 March 2016

Received in revised form 24 April 2016

Accepted 1 May 2016

Available online 7 May 2016

Keywords:

Solar heating

Heat pumps

PV

PVT

FPC

ABSTRACT

Using solar energy for space heating purposes consists an alternative way for substituting fossil fuel and grid electricity consumption. In this study, four solar assisted heat pump heating systems are designed, simulated and evaluated energetically and financially in order to determine the most attractive solution. The use of PV collectors with air source heat pump is compared to the use of FPC, PVT and FPC with PV coupled with a water source heat pump. A sensitivity analysis for the electricity cost is conducted because of the great variety of this parameter over the last years. The final results proved that for electricity cost up to 0.23 €/kW h the use of PV coupled with an air source heat pump is the most sustainable solution financially, while for higher electricity prices the coupling of PVT with an water source heat pump is the best choice. For the present electricity price of 0.2 €/kW h, 20 m² of PV is able to drive the air source heat pump with a yearly solar coverage of 67% leading to the most sustainable solution. Taking into account energetic aspects, the use of PVT leads to extremely low grid electricity consumption, fact that makes this technology the most environmental friendly.

© 2016 Elsevier Ltd. All rights reserved.

1. Introduction

The role of energy becomes increasingly important to fulfil the needs of modern societies and to follow the fast economic and industrial growth worldwide. Growing global concern regarding climate change motivates the governments to create specific legislation about energy policy. For European Union members, the greenhouse gasses emissions and energy consumption should have been reduced by 20% up to 2020 in order to meet the Directive 2009/28/EC [1,2]. Energy consumption in Building sector is about the 1/3 of the worldwide energy consumption, fact that proves the high importance of reducing the energy consumption in buildings [3,4].

The use of renewable energy sources in buildings is a promising way for diminishing the fossil fuel and the electricity consumption as a result to mitigate the environmental problems [5,6]. Solar energy utilization for covering building energy needs becomes more and more an attractive idea because it has high availability and it is able to be captured with simple and low cost devices. Flat plat collectors (FPC) and Photovoltaic (PV) modules are the most established solar energy conversion devices for producing useful heat and electricity respectively. The conjugation of these technologies is able to cover all the energy needs of each building.

Especially for countries with adequate solar energy potential, as Mediterranean countries, solar energy utilization is a determining factor to reach the energy goals that were set by EU. Greece with a yearly solar potential of about 1600 kW h/m² [7] is among the top 10 countries in solar energy utilization in building sector, mainly for domestic hot water production (DHW) [8]. The next step for enforcing the solar energy exploitation is to apply the solar energy systems for other proposes as space heating and cooling in order to minimize the grid electricity and the fossil fuel consumption. By using different solar collectors, the solar energy is able to be transformed to different kinds of energy. An innovative collector known as PVT (Photovoltaic thermal collector) produces electricity and useful heat simultaneously and it is a promising technology for the building sector.

Heat pump is a technology that gains more and more attention over the last years because of its low electricity consumption. Especially in Greece, the substitution of conventional boiler heating systems with heat pumps is usual because of the high fossil fuel cost. The next step is to combine solar energy utilization with heat pump creating environmentally and financially sustainable systems. The idea of using the solar energy to drive a heat pump is similar to the ground source heat pumps. The difference in the solar assisted systems is the lower initial cost [9] and for this reason in the areas with high solar energy potential, solar systems are preferred.

* Corresponding author.

E-mail address: bellose@central.ntua.gr (E. Bellos).

Nomenclature

A	area (m ²)	c	collector
b	temperature coefficient of cell (K ⁻¹)	$cell$	PV cell
C	cost (€)	e	edge
c_p	specific heat capacity (J/kg K)	el	electrical
E	energy (kW h)	$grid$	grid electricity
f	electrical solar coverage	h	hot
F	collector fin efficiency	$heat$	heating
G_T	solar irradiation on titled surface (W/m ²)	hot, in	inlet hot
H	daily solar energy (kW h/m ²)	hot, out	outlet hot
I	current (A)	in	inlet
k	thermal conductivity (W/m K)	l	load
K_{el}	specific electricity cost (€/kW h)	$load, in$	inlet load
m	mass flow rate (kg/s)	$load, out$	outlet load
M	water mass (kg)	$loss$	thermal loss
N	project life (years)	max	maximum
P	power (kW)	mp	maximum power
Q	heat (kW)	out	outlet
r	discount factor	r	reference
T	temperature (°C)	s	solar
U	heat loss coefficient (W/m ² K)	$source$	heat source
V	voltage (V)	st	storage tank
V_T	storage tank volume (m ³)	T	tank
		th	thermal
		tot	total
		u	useful
<i>Greek letters</i>		<i>Abbreviations</i>	
α	plate absorbance	COP	coefficient of performance
β	collector slope (°)	FPC	flat plate collector
ε_p	plate emittance	HP	heat pump
η	efficiency	NOCT	nominal operating cell temperature
ρ	density (kg/m ³)	PV	photovoltaic collector
τ	cover transmittance	PVT	thermo-photovoltaic collector
<i>Subscripts and superscripts</i>		TMY	typical meteorological year
am	ambient		
b	back part of the collector		

In the literature there are numerous studies related to solar energy and heat pump coupling. Air source heat pump, ground source heat pumps, solar assisted heat pumps and dual source heat pumps have been compared and tested for various climates. First of all, it essential to state that the water source heat pumps (solar and ground) performs better than air source heat pumps. More specifically, the coefficient of performance (COP) in water source heat pumps is about 4–5 [10], while for air source heat pumps is approximately 3 [11]. Moreover, Sun et al. [12], compared a solar assisted heat pump heating system with an air source heat pump and concluded that the first performs better in all weather conditions.

Many studies have focused on the combination of solar energy with ground source heat pump in order to achieve a high COP the days with high solar irradiation. Mehrpooya et al. [13] and Zhu et al. [14] studied this system with FPC and both concluded to a yearly COP of about 4.2. Dual source heat pumps which use hot water and ambient air energy have been also studied from many researchers. Chargui and Sammouda [15] used TRNSYS to simulate a residential house coupled with a dual source heat pump and concluded that a higher temperature of hot water improves the performance of the system and can give COP values greater than 6. Wang et al. [16] studied a novel solar PVT air dual-heat-source composite heat pump hot water system. In this system, ambient air and hot water are the heat sources for the heat pump which finally proved to have a satisfying efficiency. The COP was calculated to be ranged from 3 to 4, performing better than usual air source heat pumps.

The use of PVT with heat pumps is not usual in literature; however some interesting studies have been conducted. Tsai [17] studied an innovative PVT heat pump system for hot water production. The collector is the evaporator of the system and the condenser is located inside the hot water storage tank. The final results proved very good operation of this system with the electricity output from PVT to be adequate for the compressor needs. Good et al. [18] examined various solar collector systems in order to achieve zero energy consumption for a single family building in Norway. The studied systems were a combination of solar thermal and PV, a combination of covered PVT and PV, and a system with only PV. The final results proved that the system with only PV is the one that gets closest to reaching net zero energy balance. Calise et al. [19] studied with TRNSYS a polygeneration system using PVT coupled with heat pump and adsorption chiller for producing heating, cooling, domestic hot water and electricity. The optimum collecting area was proved to be about 25 m² and this system can be financially feasible when the initial cost will be reduced about 50%. Moreover, the use of PVT with water source heat pumps has been referred as a promising technology from other researchers [20,21].

In other studies, solar assisted heat pump systems with FPC have been analyzed successfully. Kuang et al. [22] investigated the thermal performance of a solar assisted heat pump system with FPC and water storage tank during the winter in north China. Svard et al. [23] described a new design procedure for solar assisted heat pump systems for space heating purposes. They sta-

ted that the heat pump capacity is an important parameter of the system and it significantly affects the total system performance. Furthermore, Cai et al. [24] studied a novel indirect expansion solar assisted heat pump system for space heating, cooling and domestic hot water production. More specifically, a parametric analysis was presented in order to explain the impact of ambient temperature, solar irradiation, and mass flow rate in the system performance. Another important part of the research have been focused on the direct expansion solar assisted heat pumps [25,26].

The use of evacuated tube collectors with a water source heat pump studied by Çağlar and Yamalı [27] and the final results proved that COP is approximately 6. This is a high cost system that can be applied in regions with difficult winter conditions, where the heating load is high and the energy saving will be greater. The use of PV with heat pumps is analyzed less than the other solar collectors because these collectors do not produce useful heat. However, Ochs et al. [28] investigated the optimum share of PV and solar thermal collectors in combination with air sourced heat pumps or ground water heat pumps. They finally concluded that the building storeys, the electricity price and the PV cost are parameters that influence on this comparison.

In this study, the use of FPC, PV and PVT collectors with heat pumps is analyzed. Four systems are presented and examined energetically and the system performance is presented for a range of collecting areas in each case study. The financial sustainability of every system is a decision parameter and for this reason a basic financial evaluation is presented in this study. A sensitivity analysis toward electricity cost takes place because this parameter varies a lot over the last years, especially in Greece. More specifically, PV coupled with an air source heat pump, FPC with a water source heat pump, PVT with water source heat pump and the combination of PV–FPC with a water source heat pump are the examined systems which are compared. This study comes to resume all the usual solar assisted heat pump systems, something that that is not clearly presented in the current literature.

The present work is a simulation with Transient System Simulation Tool (TRNSYS) which provides many features to the user for simulations of solar energy systems. Many parameters of the examined systems are determined from the TRNSYS default values. The examined solar collectors, heat pumps and the other devices are taken from the TRNSYS libraries, something that is very common in numerous simulations up to time.

2. Examined cases and theory

2.1. Theoretical background

It is essential to define the parameters of the present analysis. These are related to efficiency performance of the system and to the cost evaluation of every investment. The main parts of the examined systems are solar collectors (PV, FPC, PVT), heat pumps (air and water source) and other storage devices (storage tank and batteries).

Heat pump efficiency is determined by coefficient of performance (C.O.P.) which is defined as the ratio of produced heating (Q_{heat}) to electricity (P_{el}) consumed, according to Eq. (1). This parameter is depended on the temperature level of the input heat source, something that is analyzed more detailed in Section 2.4.

$$COP = \frac{Q_{heat}}{P_{el}}, \quad (1)$$

The energy utilization in every system is calculated by using the electrical solar coverage (f) which determined as the electricity produced by solar collectors to the demanded energy (P_{tot}). This

parameter can be calculated by an indirect way by taking into account the energy that consumed from the grid (P_{grid}), according to Eq. (2):

$$f = 1 - \frac{P_{grid}}{P_{tot}}, \quad (2)$$

The available solar energy (Q_s) is equal to the product of solar collector aperture and of solar incident irradiation in the title surface (G_T), according Eq. (3):

$$Q_s = A_c \cdot G_T, \quad (3)$$

The efficiency determination of every solar collector is made by a different way because the useful output in every case is different. For flat plate collectors (FPC) the useful output is the heat absorbed by the working fluid (water). This efficiency is characterized as thermal (η_{th}) and given by the next equation:

$$\eta_{FPC} = \eta_{th} = \frac{Q_u}{Q_s} = \frac{\dot{m} \cdot c_p \cdot (T_{out} - T_{in})}{Q_s}, \quad (4)$$

For photovoltaic collectors (PV) the useful output is electricity and for this reason their efficiency is electrical efficiency (η_{el}) as Eq. (5) presents:

$$\eta_{PV} = \eta_{el} = \frac{P_{el}}{Q_s} = \frac{I_{mp} \cdot V_{mp}}{Q_s}, \quad (5)$$

For thermo-photovoltaic collectors (PVT) there are two useful outputs; electricity and thermal energy. Eq. (6) presents the total efficiency of this collector which is equal to the sum of the useful outputs to the available solar energy to the collector aperture.

$$\eta_{PVT} = \eta_{el} + \eta_{th} = \frac{P_{el} + Q_{th}}{Q_s}, \quad (6)$$

In the comparison of heating technologies, financial analysis is essential in order to determine the more feasible solutions. A simple way to compare the examined cases is to calculate the total cost of every investment in the present economical basis. This is similar as net present value or better “net present cost”. Eq. (7) gives the total cost (C_{TOTAL}) as the sum of the capital cost of every investment ($C_{CAPITAL}$) and of the variable cost for all the investment years ($C_{VARIABLE}$). Eq. (8) shows the way that the variable cost is calculated, which is mainly the cost of consumed grid electricity. This cost is the product of the yearly energy consumed by the grid (E_{grid} [kW h]) and of the specific electricity cost (C_{el} [€/kW h]).

$$C_{TOTAL} = C_{CAPITAL} + C_{VARIABLE}, \quad (7)$$

$$C_{VARIABLE} = \sum_{k=1}^N \frac{E_{grid} \cdot K_{el}}{(1+r)^k}, \quad (8)$$

2.2. Examined building

The examined building is a building with main dimensions (10 m × 10 m × 3 m). The four external walls are located to four directions and double windows are placed to south, west and east side with area of 6 m², 3 m² and 3 m² respectively. Usual values for the internal gains have been taken into consideration. More specifically, the equipment load is about 1.5 kW, the lighting load is 1 kW and 10 seated persons have been taken into account for this analysis [10]. The building is supposed to be a commercial building which operates from 8:00 to 18:00 daily. The ventilation of the building is supposed to be three air changes per hour. The analysis is conducted for months with heating load and more specifically from November to April. Table 1 includes the main data of the examined building.

The layers of the structural components have a great impact on the final heating loads. The existence of insulation is a factor that

Table 1
Building parameters.

Parameters	Values	Parameters	Values
Floor area	100 m ²	Equipment load	1.5 kW
Height	3 m	Persons	10
Indoor thermal capacitance	720 kJ/K	Lighting load	1.0 kW
East double window	3 m ²	Ventilation rate	3 changes/h
West double window	3 m ²	Operation program	8:00–18:00
South double window	6 m ²	Windows U-value	1.4 W/m ² K

reduces the loads up to 3 times. The insulation of the presented building is good enough and this fact results to relative low heating demand. The external walls have a total thickness of 35 cm with the following layers: 1.5 cm plaster, 12 cm brick, 8 cm insulation, 12 cm brick and 1.5 cm plaster. Roof thickness is 31.5 cm with the following composition: 20 cm cement, 10 cm insulation and 1.5 cm plaster (internal side). The ground floor has various layers from cement and insulation materials with a total thickness of 40 cm and thermal transmittance (*U*-value) equal to 0.31 W/m² K. The external walls, the roof and the windows have *U*-values equal to 0.406 W/m² K, 0.36 W/m² K and 1.4 W/m² K respectively. The last important information for the full determination of the building is the thermal properties of the structure materials. Table 2 gives the information about thermal conductivity, specific heat capacity and density of the used materials.

The heating load of the building is calculated by TRNSYS easily and it is depended on the desired temperature inside the building. Fig. 1 shows the monthly heating loads of the examined building for various values of indoor desired temperature. In this study, 22 °C was selected as the preferable indoor temperature level in order to achieve usual thermal comfort conditions. Table 3 gives the monthly loads and the total heating loads for the selected indoor temperature level of 22 °C. The total winter load is 4998 kW h and the month with the maximum load is January with 1209 kW h. The ratio of this heating load to building area is about 50 kW h/m² and it is in accordance with Papakostas et al. study [29] for Athens.

Fig. 2 depicts the ambient temperature and the mean daily solar energy delivered to the horizontal surface for the examined months. The ambient temperature is minimum in January and the solar irradiation is minimum in December. These data can explain the reason that the January heating load is the maximum one. The solar irradiation is minimum in December because the winter solstice is observed in this month.

2.3. Examined solar collectors

Three different collector types are used in this study; photovoltaic collectors, flat plate collectors and thermal–photovoltaic collectors. The efficiencies curves of these collectors calculated by TRNSYS are presented below because they determine the energetically performance of the system. In the majority of the selected parameters, the default values from TRNSYS databases were used in order to examine typical solar collectors.

2.3.1. Photovoltaic module

Photovoltaic collectors or modules use solar energy in order to produce electricity. Their efficiency is influenced on ambient tem-

Table 2
Thermal properties of structural materials.

Material	<i>k</i> (W/m K)	<i>c_p</i> (J/kg K)	<i>ρ</i> (kg/m ³)
Brick	0.85	1000	1800
Plaster	1.40	1000	2000
Insulation	0.04	800	40
Concrete	2.00	800	2400

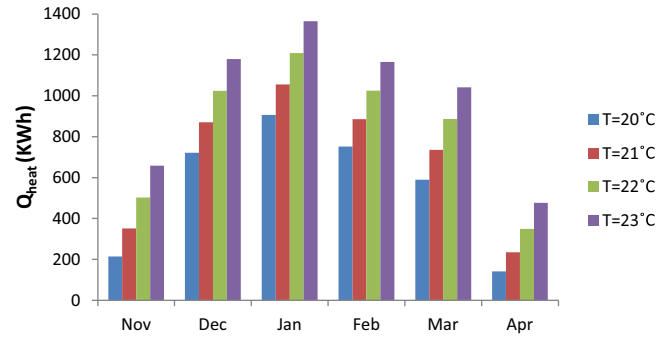


Fig. 1. Monthly heating loads of the examined building depended on the indoor desired temperature level.

perature and on solar irradiation delivered to the collector aperture. Fig. 3 illustrates the *I*–*V* curve of the examined collector at reference conditions. The maximum produced power is approximately 100.4 W at reference conditions. Moreover, Table 4 gives all the characteristics of the examined PV module. The aperture of the module is 0.89 m² and in order to achieve great collecting area more modules are placed in parallel series.

2.3.2. Flat plate collector

The next examined solar collector is a usual selective flat plate collector which produces useful heat. Fig. 4 shows the thermal efficiency of this collector as a function of parameter $[(T_{in} - T_{am})/G_T]$ which is a typical parameter for expressing the solar collector performance. Eq. (9) is a good approximation of this curve with the least square method.

$$\eta_{th} = 0.8 - 3.61 \cdot \left(\frac{T_{in} - T_{am}}{G_T}\right) - 13.889 \cdot \left(\frac{T_{in} - T_{am}}{G_T}\right)^2, \quad (9)$$

2.3.3. Thermo-photovoltaic collector

The last presented solar technology is a thermal–photovoltaic collector which produces electricity and useful heat simultaneously. The performance of this collector is fully depended on the operating temperature level of the cell. Eq. (10) shows how the electrical efficiency of the module changes for different cell temperature levels:

$$\eta_{el}(T_{cell}) = \eta_{el,max} \cdot (1 - b \cdot (T_{cell} - T_{ref})), \quad (10)$$

Table 5 gives the main parameters of the examined PVT module as they used in the simulation tool [30]. Fig. 5 depicts the efficiencies of this collector as a function of the parameter $[(T_{in} - T_{am})/G_T]$. This parameter influences on the electrical efficiency because the cell temperature is depended by the operating conditions (water inlet temperature, ambient temperature and solar radiation level). Eqs. (11)–(13) give the electrical thermal and total PVT efficiencies respectively. These formulas are approximately given the performance of the examined PVT module and they have been made by TRNSYS simulation. It is interesting that the slope of the thermal efficiency curve is high, fact that proves the low thermal efficiency of the PVT module in high water temperature levels.

$$\eta_{el} = 0.1286 - 0.3269 \cdot \left(\frac{T_{in} - T_{am}}{G_T}\right), \quad (11)$$

$$\eta_{th} = 0.6853 - 11.294 \cdot \left(\frac{T_{in} - T_{am}}{G_T}\right) - 44.25 \cdot \left(\frac{T_{in} - T_{am}}{G_T}\right)^2, \quad (12)$$

$$\eta_{tot} = 0.8139 - 11.6209 \cdot \left(\frac{T_{in} - T_{am}}{G_T}\right) - 44.25 \cdot \left(\frac{T_{in} - T_{am}}{G_T}\right)^2, \quad (13)$$

Table 3
Monthly heating loads of the examined building.

November 503 kW h	December 1024 kW h	January 1209 kW h	February 1025 kW h	March 887 kW h	April 349 kW h	Total 4998 kW h
----------------------	-----------------------	----------------------	-----------------------	-------------------	-------------------	--------------------

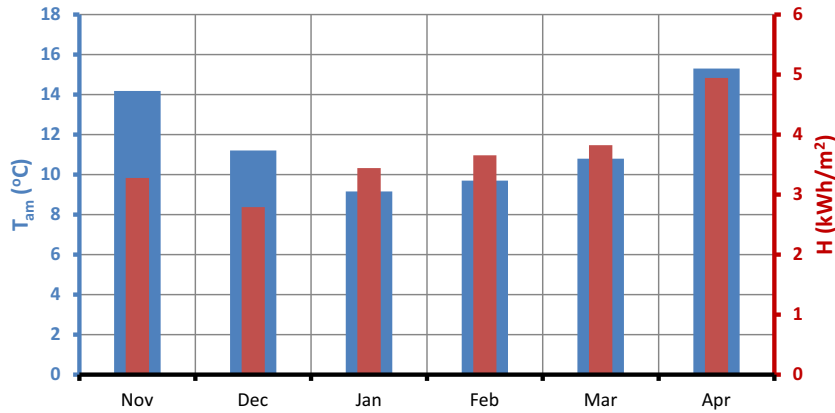


Fig. 2. Ambient temperature and daily solar energy on horizontal for the mean day of the examined months.

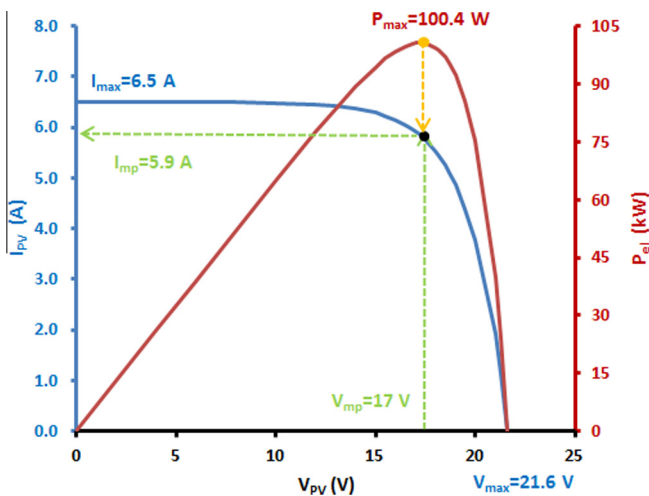


Fig. 3. PV module performance at reference conditions ($T_{cell} = 25\text{ °C}$ and $G_T = 1000\text{ W/m}^2$).

Another important parameter is the cell temperature of the PV part. This temperature influences on the electrical and thermal efficiency. Fig. 6 shows the cell temperature and the water inlet temperature as a function of the parameter $[(T_{in} - T_{am})/G_T]$. It is obvious that for higher water inlet temperature levels, the difference between the presented temperatures is getting lower something that mainly deals with the decrease in thermal efficiency of the collector.

Table 4
Properties of the used PV module.

Parameters	Values	Parameters	Values
I_{max} (at ref)	6.5 A	Module temperature at NOCT	40 °C
V_{max} (at ref)	21.6 V	Ambient temperature at NOCT	20 °C
I_{mp} (at ref)	5.9 A	Insolation at NOCT	800 W/m ²
V_{mp} (at ref)	17 V	Temperature coefficient of I_{max}	0.02 A/K
T_{ref}	25 °C	Temperature coefficient of V_{max}	-0.079 V/K
$G_{T,ref}$	1000 W/m ²	Semiconductor bandgap	1.12 eV
A_{pv}	0.89 m ²	Transmittance absorbance product	0.95

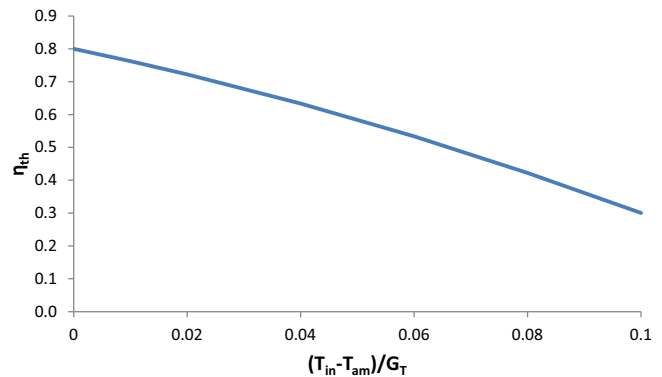


Fig. 4. Thermal efficiency curve of flat plate collector as a function of operation conditions.

2.4. Performance of the examined heat pumps

Two kinds of heat pumps are used in this study. The first one is an air source heat pump (air to air) which produces hot air from the environment heat sink. The second is a water source heat pump (water to air) which uses hot water heat sink in order to produce hot air. The water source heat pump needs an extra heat source which is the solar energy in the examined cases. Fig. 7 depicts the coefficient of performance of the utilized heat pumps from the TRNSYS data base. The main parameter of the COP is

Table 5
Properties of the used PVT collector.

Parameters	Values
Fin efficiency (F)	0.968
Plate absorbance (α)	0.9
Cover transmittance (τ)	0.95
Plate emittance (ϵ_p)	0.1
Edge and back heat loss coefficient ($U_e + U_b$)	0.8 W/m ² K
Maximum cell efficiency at reference temperature	15%
Temperature coefficient of cell efficiency (b)	0.0045 K ⁻¹
Temperature for cell reference efficiency	25 °C

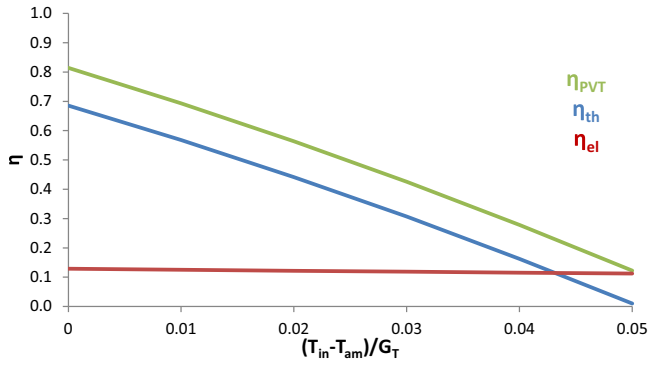


Fig. 5. Thermal, electrical and total efficiency of the examined thermo-photo-voltaic collector.

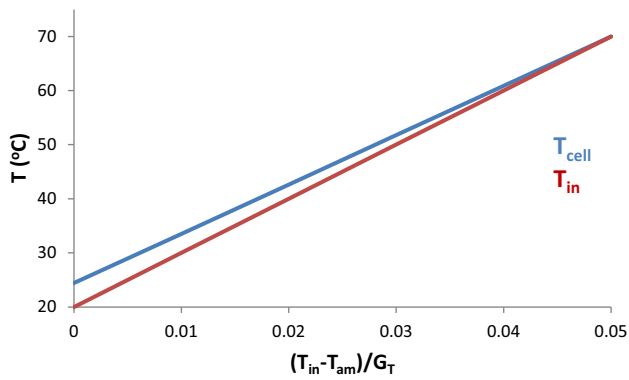


Fig. 6. Comparison of PV-cell and water inlet temperature for various operating conditions.

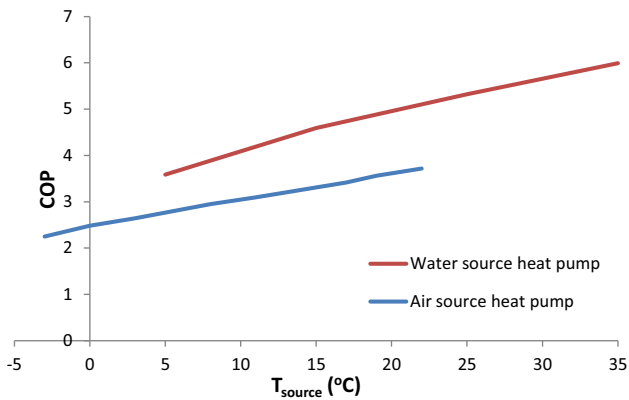


Fig. 7. Air source and water source heat pump heating performance for various values of heat source temperature.

the heat source temperature which is the horizontal axis in Fig. 6. As it is obvious, water source heat pump performs but need higher source temperature levels than air source heat pump. Moreover, Table 6 gives the main parameters used in TRNSYS for each heat pump.

2.5. Storage devices

2.5.1. Thermal storage

A storage tank of hot water is used in order to store the supplementary solar energy during the day. Fig. 8 shows the modeling of

Table 6
Air and water source heat pumps parameters.

Parameters	Heat pump	Values
Indoor fan power	Both	190 W
Fraction of outside air	Both	15%
Working fluid temperature (UA) between working fluid and indoor air	Water	55 °C
Outdoor fan power	Air	207 W
Volumetric flow rate of hot air	Both	500 l/s

$$Storage = Input - Output - Losses$$

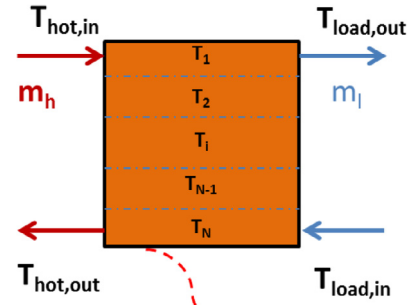


Fig. 8. Storage tank modelling.

the examined storage tank. According this modeling, there are “N” mixing zones and temperature (T_i) is uniform in every zone “i”. An energy balance is made in every zone and finally a system of N differential equations is created [31]. The basic idea of the energy balance in every zone is the given by the following equation:

$$Storage = Input - Output - Losses$$

The storage tank energy equations are presented below (Eqs. (14)–(17)). Eq. (14) is the energy balance in the first node, Eq. (15) is for the random node “i” and Eq. (16) for the last node “N”. The total thermal losses of the tank (Q_{loss}) are the sum of the losses of all the nodes according Eq. (17). These thermal losses include radiation and convection heat losses.

$$M_1 \cdot c_p \cdot \frac{\partial T_1}{\partial t} = \dot{m}_h \cdot c_p \cdot (T_{hot,in} - T_{ST1}) + \dot{m}_l \cdot c_p \cdot (T_2 - T_1) - U_T \cdot A_{ST,1} \cdot (T_1 - T_{am}), \quad (14)$$

$$M_i \cdot c_p \cdot \frac{\partial T_i}{\partial t} = \dot{m}_h \cdot c_p \cdot (T_{i-1} - T_i) + \dot{m}_l \cdot c_p \cdot (T_{i+1} - T_i) - U_T \cdot A_{ST,i} \cdot (T_i - T_{am}), \quad (15)$$

$$M_N \cdot c_p \cdot \frac{\partial T_N}{\partial t} = \dot{m}_h \cdot c_p \cdot (T_{N-1} - T_N) + \dot{m}_l \cdot c_p \cdot (T_{load,in} - T_N) - U_T \cdot A_{ST,N} \cdot (T_N - T_{am}), \quad (16)$$

$$Q_{loss} = \sum_{j=1}^N [U_T \cdot A_{ST,j} \cdot (T_j - T_{am})], \quad (17)$$

The outer area and the water mass of every zone are symbolized with $A_{ST,i}$ and M_i respectively. The thermal loss coefficient (U_T) is equal to 0.8 W/m² K for this study, a typical value for insulated tanks. The height of every node is taken equal to 0.2 m and generally 6 nodes are used in every tank model. The use of more nodes increases the calculation time with no effect on the final results.

2.5.2. Electricity storage

Batteries are used in the simulation for storing the electricity produced by PV and PVT modules. The storage capacity of the batteries is depended on the installed power in every case. Table 7 shows the battery parameters used in the simulations.

2.6. Other used components

In the simulations of the examined systems many other components are used in order to simulate properly every case. In this section the main information about control systems, water pumps and inverters are given.

The control system has a one level thermostat which is regulated at 22 °C. The dead band is about 0.5 °C and 5 oscillations are permitted in every time-step. The water pump practically is used for determining the flow rate of every stream. The inverter that used in the system is a very important component because determine the power consumed by the grid. Table 8 gives the main parameters of the used inverter in the examined systems.

3. Examined systems

In this paragraph the examined systems and the methodology of the analysis are presented. The simulation tool is TRNSYS which offers a great variety of features to the users. Four different solar heating systems are presented and compared energetically and financially in order to determine the most feasible solution.

3.1. Simulation process and methodology

TRNSYS is a transient simulation program which simulates complex systems. The examined systems consist of properly connected components (types). Every component (type) has its own executable program which runs in the background of the TRNSYS. The user has to regulate many parameters and to connect them properly between components in order to simulate the system with a suitable way. The utilized types on the examined systems are given in Table 9.

It is essential to state that the time-step in all the simulations is 0.05 h (=12 min) and this time-step was selected after testing the performance of the systems in various time-steps. The simulation period is the winter period from November to April and the respective yearly hours are 7297–11,640. TRNSYS solves the differential equations with the modified Euler method while the non-linear equations are solved with successive method because there is building in the simulation, according manual directions. Weather data was taken for typical meteorological year (TMY) in Athens and for the diffuse radiation was used the Perez-model [32]. This model is a complex model which accounts for circumsolar, horizon brightening and isotropic diffuse radiation. The ground reflectance was selected to be equal to 0.2 which is used for typical ground.

In every system, a simple sensitivity analysis takes place in order to examine the system performance in various combinations

Table 7
Battery parameters.

Parameters	Values
Charging efficiency	90%
Maximum charge voltage per cell	2.5 V
Maximum current per cell charging	3.33 A
Maximum current per cell discharging	−3.33 A
Cell energy capacity	15–180 A h
Cells in series	6
Cells in parallel	1

Table 8
Inverter parameters.

Parameters	Values
Regulator efficiency	85%
Inverter efficiency	95%
Power capacity	3 kW
Charge to discharge limit on fractional state of charge	0.85

Table 9
Components and TRNSYS types used in simulations.

Component	TRNSYS type
Flat plate collector	1b
Water pump	3b
Storage tank	4b
Operation program	14 h
Quantity integrator	24
Psychometrics	33
Battery	47b
Inverter	48b
Thermal-photovoltaic collector	50b
Periodic integrator	55
Multi-zone building	56
Online plotter	65
Sky temperature	69
Photovoltaic module	94a
Weather data	109
Water source heat pump	505a
Air source heat pump	665-3
Heating controller	671
Calculations	Equator

of important parameters. More specifically the main parameter is the collecting area in every system which determines the solar energy coverage and the capital cost of the system. Moreover, the storage capacity of each system changes for different collecting area values. Other parameters as the mass flow rate in every circuit are selected to have values which reduce the grid electricity consumption.

3.2. Air source heat pump with PV modules

The first examined system uses an air source heat pump for space heating proposes. The electricity demand of this heat pump is covered partially by photovoltaic panels and by grid electricity consumption. An inverter and batteries are used in this system in order to convert and regulate the voltage and to store the momentary supplementary energy. Fig. 9 depicts the examined system. In order to predict the suitable slope of the collectors, an optimization of the slope angle is presented in Fig. 10. The final results prove that 45° is the optimum slope for the winter period which is examined in this study. This figure shows the energy delivered to a titled surface, so these results can be adopted to all the examined collectors.

Storage capacity of the system is very important for the optimum design of the system. This parameter is conjugated with the collecting area of the PV and for this reason greater storage capacity was used for greater collecting area. Fig. 11 depicts the dependence of these parameters in this analysis.

3.3. Water source heat pump with FPC

The idea of coupling a water source heat pump with flat plate collectors (FPC) is also examined in this study. The high water temperature makes the heat pump to perform better consuming lower amounts of electricity. A water storage tank is used in this system

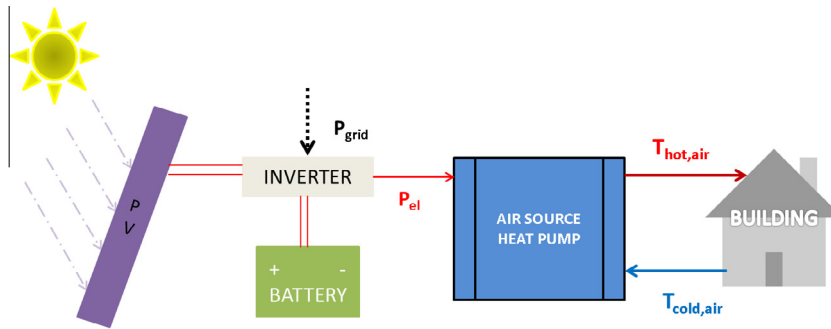


Fig. 9. Air source heat pump heating system coupled with PV modules.

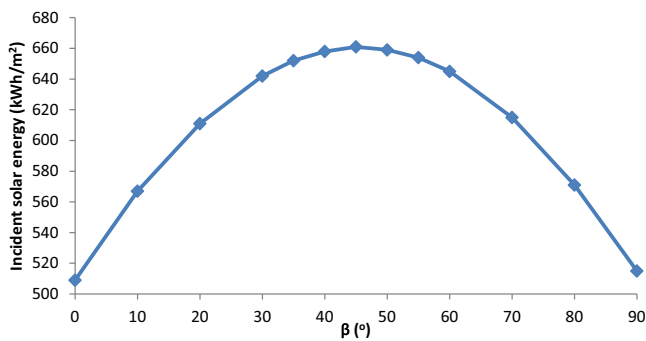


Fig. 10. Slope optimization of the PV module.

in order to store thermal energy. Fig. 12 depicts the examined system which includes FPC, storage tank, water source heat pump and building. The surface area of the FPC and the volume of storage tank are parameters that investigated in this analysis for determining the optimum operation of this heating system. The slope of the collectors is selected to be 45°, as in the case of PV modules (Fig. 10). The specific mass flow rate in the collector loop selected to be 0.0166 kg s⁻¹ m⁻² [33] and the same mass flow rate was selected to the circuit between tank and heat pump.

3.4. Water source heat pump with PVT

Thermal photovoltaic collectors combine thermal and electricity production and it is an ideal solution for feeding a water source heat pump with these quantities. This idea is examined in this study because it is of high interest due to energetic complementarity between PVT and water source heat pump. Fig. 13 shows the examined system which includes PVT, storage tank, water source heat pump, batteries, inverter and building. This is complex enough because the solar collector supplies the two energy demands of the heat pump. Storage for thermal and electrical energy is used because it essential not to loss useful energy (ther-

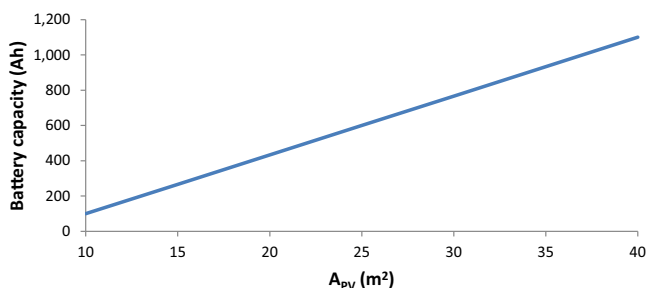


Fig. 11. Battery storage capacity as a function of PV area.

mal and electrical). The specific mass flow rate is selected to be 0.0166 kg s⁻¹ m⁻² in the collector loop, while the same mass flow rate was set in the tank-heat pump circuit. PVT slope angle is 45° something that is in accordance with Fig. 10. It is also important to be stated that the battery capacity was increased for higher PVT area in order to store all the possible produced electricity.

3.5. Water source heat pump with PV modules and FPC

The last presented system is based on the idea of feeding a water source heat pump with produced heat and electricity, as in the previous system. In this case (Fig. 14), FPC and PV are used separately and produce thermal energy and electricity for covering the heat pump respective energy needs. This idea is innovative and it is similar with the previous system. Slope angle for FPC and PV is 45° according previous optimization and the mass flow rate in water circuits is according to the previous systems.

4. Results

The results of this study are separated in 2 categories, the energetic and the financial results. Energetic results are necessary to determine the system with the lower energy consumption, while financial results aid to select the most attractive investment. In every system, a sensitivity analysis is presented in order to correlate the energy consumption with the utilized solar collector surface. The storage capacity follows the increase in solar field in order to minimize the energy waste.

4.1. Energetic performance of the examined systems

4.1.1. Air source heat pump coupled with PV

The first examined system is depicted in Fig. 9 and includes an air source heat pump coupled with photovoltaic panels. A sensitivity analysis is conducted for analyzing the system performance for various values of PV surface. In every case the power consumed from the grid is calculated and the solar coverage. Fig. 15 illustrates the impact of the PV collecting area to these parameters. It is obvious that greater PV area reduces the grid electricity consumption and increases the solar coverage. More specifically, for PV surface over 20 m², the solar coverage is high enough, fact that leads to a feasible system. Up to 20 m², the solar coverage curve is increasing linearly and after this point increases with lower rate. The behavior of the grid electricity consumption exhibits reversal behavior with a reducing rate.

4.1.2. Water source heat pump coupled with FPC

The next examined system is the coupling of a water source heat pump with flat plate collectors. In this system the collecting area and the storage tank volume are important parameters. For

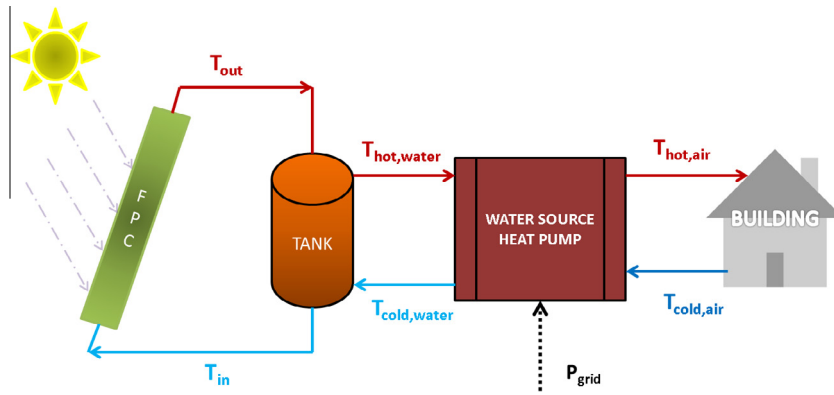


Fig. 12. Water source heat pump heating system coupled with FPC.

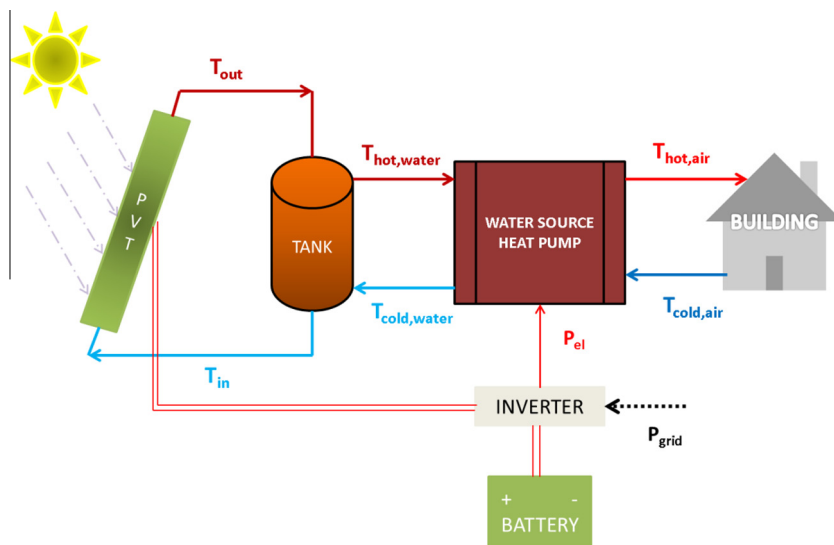


Fig. 13. Water source heat pump heating system coupled with PVT collectors.

collecting areas up to 25 m², the storage tank was selected to be 1 m³, while for higher collecting areas, a storage tank with 1.5 m³ volume was used. The impact of the storage tank volume is relative low in the results, if its values are in-between logical estimations.

In this point, it is important to state that 20 m² of FPC are needed in order to achieve an accepted profile of indoor temperature. Lower values of collecting area are not capable to deliver the needed amount of energy to the heat pump and the thermal comfort conditions are not satisfied. For this reason, Figs. 16–18 display results for collecting areas greater than 20 m². Fig. 16 shows the collectors thermal efficiency and the produced useful heat for the examined range of collecting areas. The thermal efficiency of the collector field is lower when more collectors are used because the mean operating temperature is getting greater and according to Fig. 4, the thermal efficiency is lower. This result makes the useful heat curve to increase with a reducing rate for higher collecting areas. On the other hand, the C.O.P. of the water heat pump, which is depicted in Fig. 17, increases for higher FPC surfaces because the system operates in higher temperature levels. Fig. 7 validates these results and it is proved that greater collecting surfaces aid the heat pump to operate with higher performance. Electricity consumption is getting lower with higher collecting areas, as a result of the increase in the heat pump performance. It is obvious from Fig. 17 that the collecting area up to 30 m² has essential impact of the system performance by reducing the electricity consumption and increasing the C.O.P. of the heat pump.

4.1.3. Water source heat pump coupled with PVT

The simulation results for the system of PVT and water source heat pump (Fig. 13) are presented in this paragraph. It is essential to state that 20 m² of collecting area are needed for creating and keeping the desired temperature level inside the building. For this reason, only the results for collecting areas greater than this limit are presented. Figs. 18 and 19 depict the performance of the PVT collector for every case. When greater collecting area is used, the mean operating temperature is getting greater, a fact with negative impact on the thermal efficiency and on electrical efficiency according to Fig. 5. Fig. 19 shows that the thermal and the electrical outputs have an increasing rate with greater collecting areas and the increase is approximately linear. The selected storage tank volume of the system is given in Fig. 20 and it is ranged from 1.25 m³ to 1.75 m³. Heat pump COP is depicted also in Fig. 20 and it is obvious that the greater collecting area has a positive impact on this. The COP is ranged from 5.075 to 5.85, high values which lead to low electricity consumption. Fig. 21 displays the grid electricity consumption and the solar coverage for the range of the examined collecting areas. Generally, the consumption is significant low, compared to other systems because of the produced electricity and of the high COP of the heat pump. More specifically, the solar coverage is ranged from 85% to 95% and the energy consumption from 152 kW h to 171 kW h.

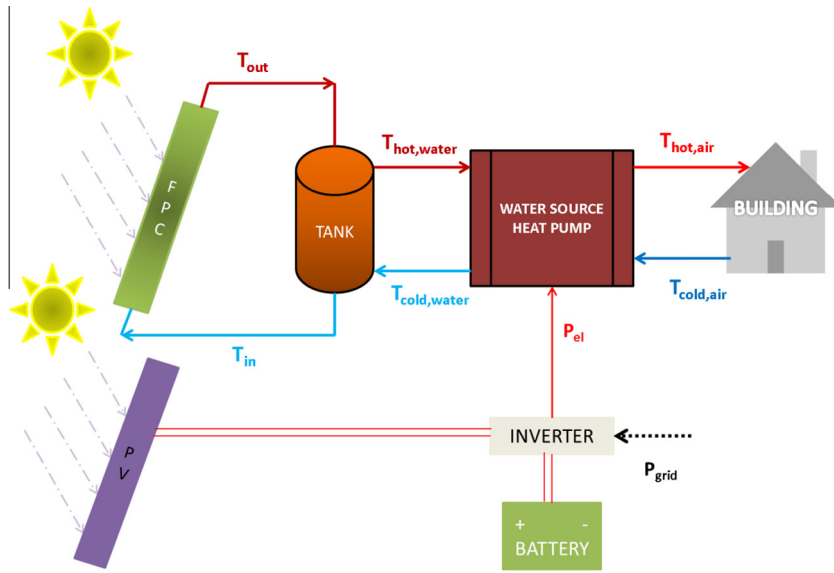


Fig. 14. Water source heat pump heating system coupled with PV modules and FPC.

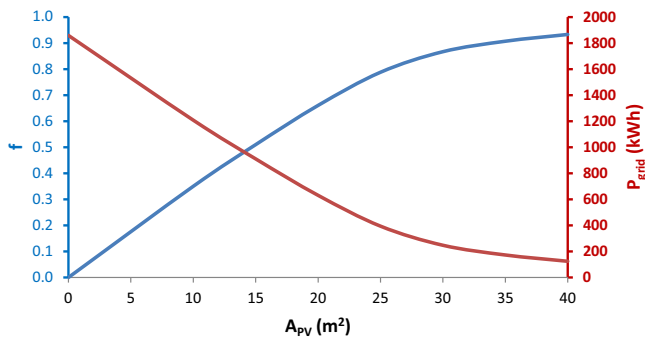


Fig. 15. Electricity consumption from grid and solar coverage for the case of PV with air source heat pump.

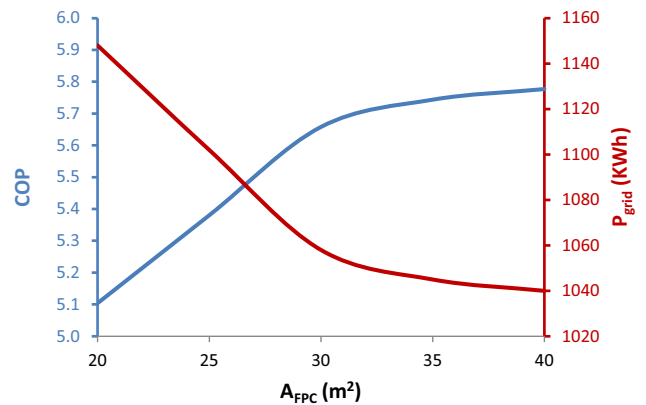


Fig. 17. COP of water source heat pump and electricity consumption from grid for the examined FPC areas.

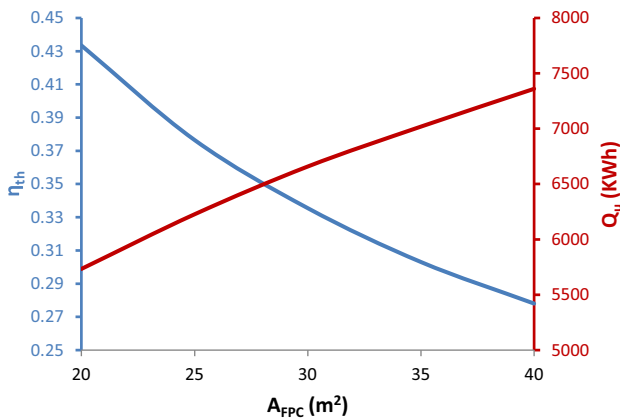


Fig. 16. FPC thermal efficiency and useful heat as a function of the collecting area in the system.

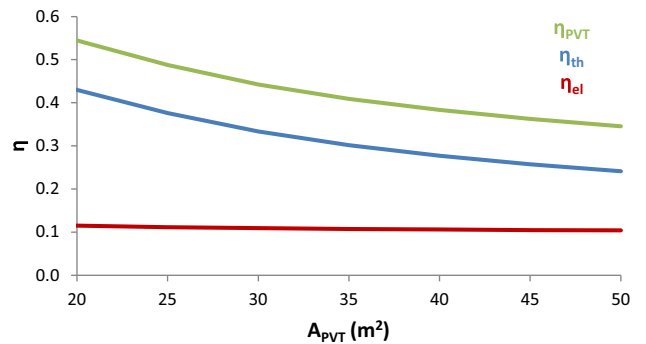


Fig. 18. Thermal, electrical and total efficiency of PVT.

4.1.4. Water source heat pump coupled with PV and FPC

The last examined system includes PV and FPC coupled with a water source heat pump. The minimum possible collecting area for FPC is 20 m² for meeting the indoor temperature limits. For this

reason 3 collecting area levels are used in the following results; 20 m², 25 m² and 30 m². Fig. 22 illustrates the grid electricity consumption and the solar coverage for various combinations of FPC and PV collecting areas. The use of greater FPC areas has a low impact on the results, fact that leads to select 20 m² of FPC as

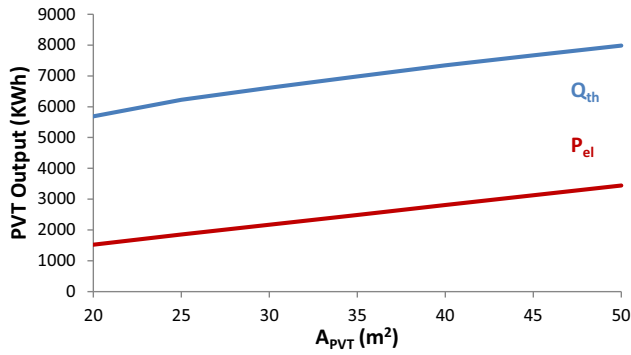


Fig. 19. Thermal and electrical output of the PVT for the examined collecting areas.

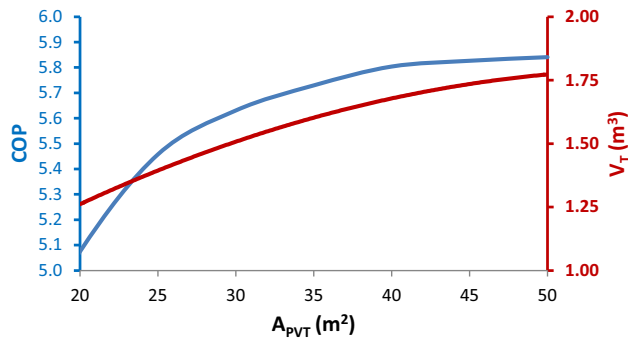


Fig. 20. COP and storage tank volume for the examined PVT surfaces.

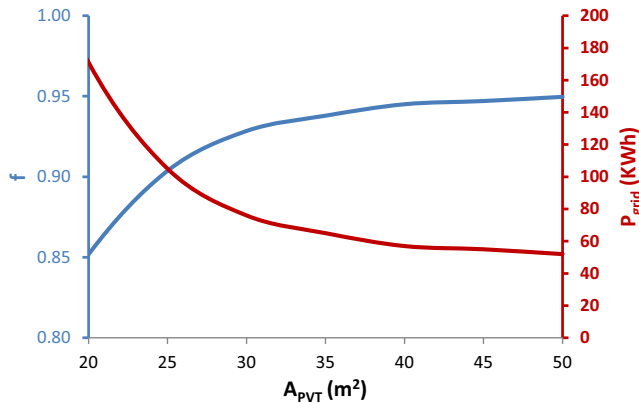


Fig. 21. Electricity consumption from grid and solar coverage for the case of PVT with water source heat pump.

the most sustainable solution. The collecting area of PV is a determining factor in the grid electricity consumption up to 30 m² collecting area. Table 10 includes the mean COP and the useful thermal energy produced by FPC. It is important to state that the mean COP takes into account all the winter period. Greater FPC area leads to higher COP because the mean water temperature in the system is higher and the heat pump operates with input energy of higher quality. The storage tank volume was selected to be 1 m³, after a simple sensitivity analysis.

4.2. Financial performance of the examined systems

The next step in this study is the financial evaluation of the examined technologies. The systems are compared by taking into

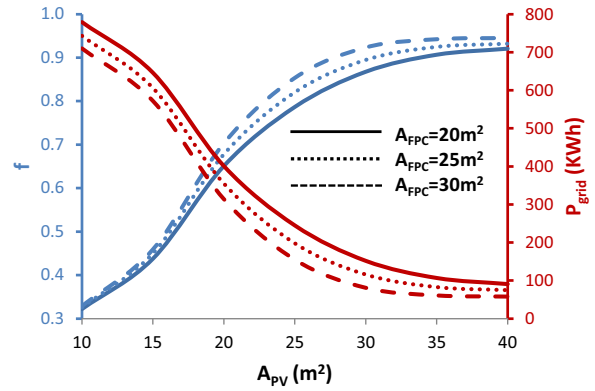


Fig. 22. Electricity consumption from grid and solar coverage for the case of FPC and PV combinations with a water source heat pump.

Table 10 System performance for various FPC areas.

A _{FPC} (m ²)	Mean C.O.P.	Q _{TH} (kW h)
20	5 · 10	5734
25	5 · 38	6227
30	5 · 66	6658

consideration the initial investment cost and the cost of grid electricity consumption for the life time of the investment. Because the specific electrical cost has not a constant value the last years, especially for Greece, a sensitivity analysis is conducted in a great range from 0.15 €/kW h to 0.3 €/kW h. At present, the electricity cost in Greece is about 0.2 €/kW h including taxes and other charges paid by the consumers. The project life and the discount factor are selected to be 25 years and 4% respectively. The low value of discount factor is explained by the financial crisis in the present years. Table 11 includes the cost or the specific cost of the used components in all the examined systems.

Figs. 23–26 illustrate the total cost of the system for the examined cases for various values of electricity cost. It is essential to explain that technologies with higher grid electricity consumption are not feasible when the electricity price is high enough. On the other hand, these systems are financially ideal for low electricity cost cases.

Fig. 23 depicts that there are optimum collecting areas for PV which minimizes the total cost of the investment. For electricity price 0.2 €/kW h, 20 m² PV collectors lead to minimum total cost which is 15,212 €. The reason for the increasing total cost after a point in every curve is explained by the reduced solar energy exploitation for higher collecting areas.

Table 11 Financial parameters of the study [34].

Parameter	Value
Project life	25 years
Discount factor	4%
PV cost	150 €/m ²
PVT cost	200 €/m ²
FPC cost	150 €/m ²
Inverter cost	1500 €
Storage tank cost	500 €/m ³
Battery cost	1 €/A h
Air source heat pump cost	7500 €
Water source heat pump cost	8500 €

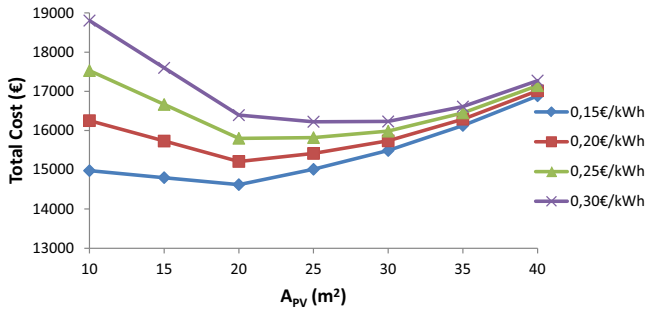


Fig. 23. Total cost of PV system with air source heat pump for the examined collecting areas and for various electricity costs.

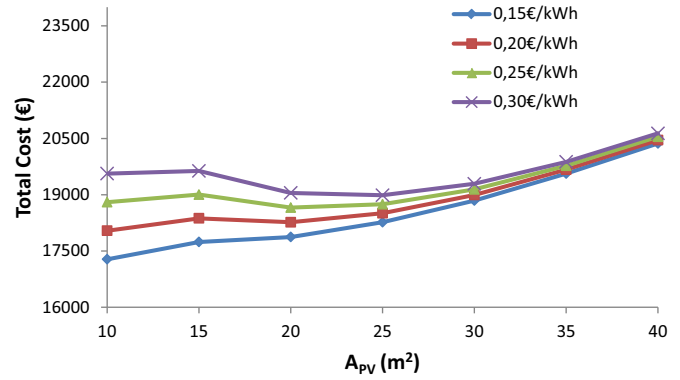


Fig. 26. Total cost of FPC and PV system with water source heat pump for 20 m² FPC area and for various electricity costs.

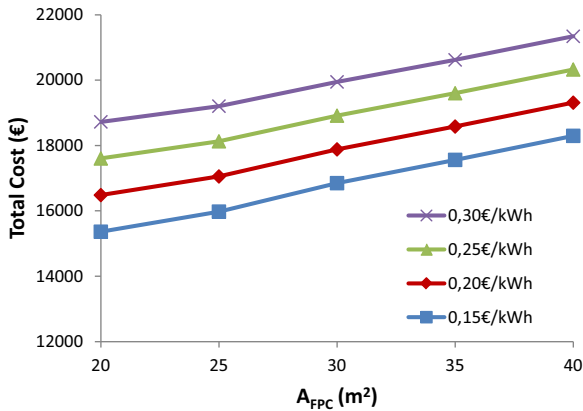


Fig. 24. Total cost of FPC system with water source heat pump for the examined collecting areas and for various electricity costs.

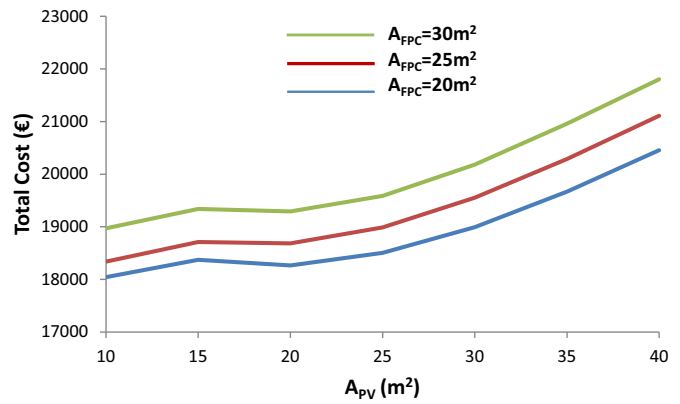


Fig. 27. Total cost of FPC and PV system with water source heat pump for the examined collecting areas for electricity cost 0.2 €/kWh.

The next examined system is a water source heat pump coupled with FPC. Fig. 24 shows the total cost of the investment for the examined cases. The results proves that the FPC area should be the lower possible in order to have lower cost. This can be explained by Fig. 17, where the impact of the FPC area in the COP is low. As it has referred in Section 4.1.2, it is not possible to use area lower than because it negative affects the indoor thermal comfort conditions.

Fig. 25 illustrates the financial results for the PVT collectors coupled with the water source heat pump. As it is depicted in this figure, all the curves are close to each other because of the low grid

electricity consumption. This result proves that this technology is preferred for areas with high electricity price. Again it is essential to say that PVT area under 20 m² does not lead to an accepted indoor micro-climate which keeps the indoor temperature over 22 °C.

The conjugation of PV and FPC with a water heat pump is the last examined system. Fig. 26 illustrates the results for various electricity prices. All the curves are calculated for 20 m² FPC area. This area is the suitable one according to Fig. 22. Fig. 27 also exhibits that the use of 20 m² FPC is the best choice financially. Moreover, Fig. 26 displays that the optimum PV area is depended on the

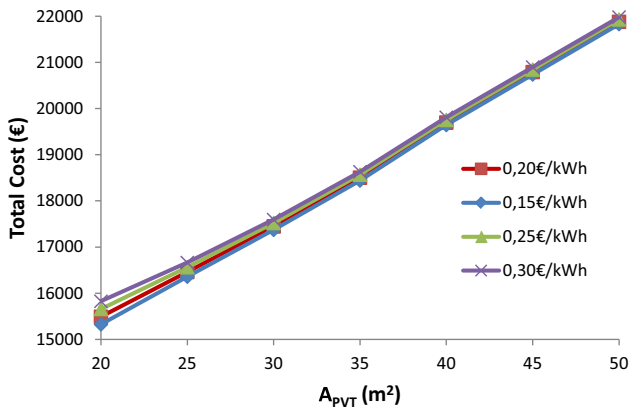


Fig. 25. Total cost of PVT system with water source heat pump for the examined collecting areas and for various electricity costs.

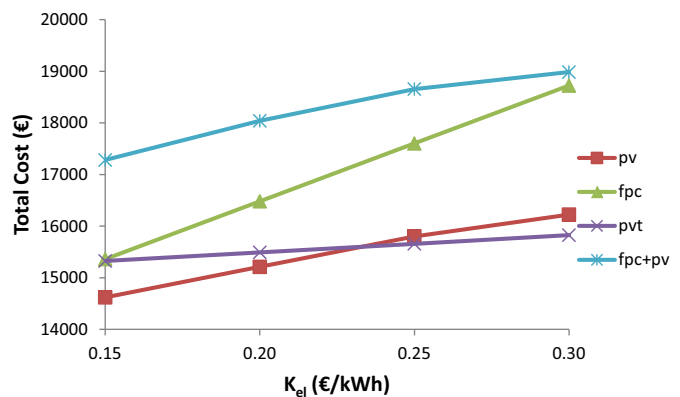


Fig. 28. Final comparison of the examined systems for various electricity costs.

Table 12
Final comparison of the examined cases.

Electricity cost (€/kW h)	Parameters	CASE 1 PV Air-HP	CASE 2 FPC Water-HP	CASE 3 PVT Water-HP	CASE 4 FPC/PV Water-HP
0.15	A (m ²)	20	20	20	20/10
	Q _{grid} (kW h)	956	1148	171	779
	Total cost (€)	14,622	15,362	15,336	17,281
0.20	A (m ²)	20	20	20	20/20
	Q _{grid} (kW h)	956	1102	171	401
	Total cost (€)	15,212	16,483	15,493	18724
0.25	A (m ²)	20	20	20	20/20
	Q _{grid} (kW h)	956	1045	171	401
	Total cost (€)	15,803	17,603	15,660	18,657
0.30	A (m ²)	25	20	20	20/25
	Q _{grid} (kW h)	605	1040	171	245
	Total cost (€)	16,225	18,724	15,827	18,985

electricity price. For the electricity price of 0.2 €/kW h, 10 m² PV area lead to minimum total investment cost.

4.3. Final comparison of the examined systems and discussion

In this point it is essential to resume all the above results in order to determine the most feasible solution. Fig. 28 and Table 12 summarize the optimum solutions for the examined electricity prices. It is obvious from Fig. 28 that for the present electricity cost (0.2 €/kW h) the system with PV and air source heat pump is the most attractive investment. However, for a greater electricity price, over 0.23 €/kW h, the system of PVT coupled with a water heat pump seems to lead to the most feasible solution. The other two systems with FPC and PV–FPC coupled with a water source heat pump are not so feasible solutions. Table 12 includes analytical information about the optimum collecting area, the grid electricity consumption and the total cost for each point case in Fig. 28.

The results of this sensitivity analysis are in fact very interesting because four innovative solar heating technologies were compared in an energetically and financially basis. The use of PV and PVT coupled with air source and water source heat pump respectively are feasible solutions. The electricity price is the deciding factor for select which technology is financially more attractive. On the hand, PVT is the collector with the lower grid electricity consumption, while the case with FPC the most grid electricity consuming. These results are summarized in Fig. 29.

Finally, for the present electricity price of 0.2 €/kW h, the use of 20 m² PV with an air source heat pump is the best choice, while 20 m² of PVT with a water source heat pump is the second one.

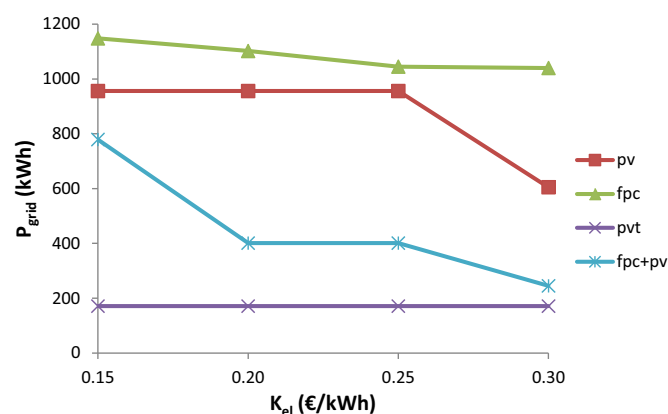


Fig. 29. Grid electricity consumption for the financially optimum cases.

However, the grid electricity consumption in the first case is 956 kW h yearly and with the second only 171 kW h yearly. This comparison proves that energetically and environmentally, the use of PVT is a very attractive solution because these collectors have double output (heat and electricity).

5. Conclusions

This study examines various solar heating systems energetically and financially. The simulation tool is TRNSYS and the examined period is from November to April. A usual building in Athens of 100 m² area is examined with a yearly heating demand of about 5000 kW h. Four heating systems are compared; an air source heat pump coupled with PV collectors, a water source heat pump coupled with FPC, a water source heat pump coupled with PVT and a water source heat pump coupled with PV and FPC together.

In the first part of this study, the systems are analyzed energetically with a parametric study based on collecting areas. Important result is that for the water source heat pumps, 20 m² of solar collectors (FPC or PVT) are needed in order the desired thermal comfort conditions to be satisfied. Solar coverage is increased for higher collecting areas and simultaneously the COP in the water source heat pump. In the financial study, the minimum total investment cost is the comparison criterion for selecting the most feasible system in every case. A sensitivity analysis is presented based on electricity price, because this parameter varies the last years.

The final results proved that for the present electricity cost of 0.2 €/kW h and up to 0.23 €/kW h the use of 20 m² PV area with an air source heat pump is the most attractive solution financially. For higher prices of electricity, 20 m² of PVT collectors coupled with a water source heat pump is the ideal choice. On the other hand, PVT system consume extremely low grid electricity, compared to other systems, and for this reason it renders the most environmental friendly solution for space heating.

Acknowledgment

The first author would like to thank ONASSIS Foundation for its financial support.

References

- [1] Michael JJ, Iniyani S, Goic R. Flat plate solar photovoltaic–thermal (PV/T) systems: a reference guide. *Renew Sustain Energy Rev* 2015;51:62–88.
- [2] Directive 2009/28/EC. On the promotion of the use of energy from renewable sources; 2009.
- [3] Wan K, Li D, Liu D, Lam J. Future trends of building heating and cooling loads and energy consumption in different climates. *Build Environ* 2011;46:223–34.

- [4] Zeng R, Wang X, Di H, Jiang F, Zhang Y. New concepts and approach for developing energy efficient buildings: ideal specific heat for building internal thermal mass. *Energy Build* 2011;43:1081–90.
- [5] Li Q, Shirazi A, Zheng C, Rosengarten G, Scott JA, Taylor RA. Energy concentration limits in solar thermal heating applications. *Energy* 2016;96:253–67.
- [6] Prasartkaew B, Kumar S. Design of a renewable energy based air-conditioning system. *Energy Build* 2014;68(A):156–64.
- [7] Kouremenos DA, Antonopoulos KA, Domazakis ES. Solar radiation correlations for the Athens, Greece area. *Solar Energy* 1985;35(3):259–69.
- [8] Mauthner F, Weiss W, Spork-Dur M. Solar heat worldwide: market and contribution to the energy supply 2013. Design, Graphics, Typesetting & Image processing: Steinhuber Info Design, Graz, Austria; edition 2015.
- [9] Emmi G, Zarrella A, De Carli M, Galgaro A. An analysis of solar assisted ground source heat pumps in cold climates. *Energy Convers Manage* 2015;106:660–75.
- [10] Bellos E, Tzivanidis C, Delis A, Antonopoulos KA. Comparison of a solar driven heat pump heating system with other typical heating systems with TRNSYS. ECOS conference 2015, Pau, France; 2015.
- [11] Cabrol L, Rowley P. Towards low carbon homes – a simulation analysis of building-integrated air-source heat pump systems. *Energy Build* 2012;48:127–36.
- [12] Sun X, Dai Y, Novakovic V, Wu J, Wang R. Performance comparison of direct expansion solar-assisted heat pump and conventional air source heat pump for domestic hot water. *Energy Proc* 2015;70:394–401.
- [13] Mehrpooya Mehdi, Hemmatabady Hoofar, Ahmadi Mohammad H. Optimization of performance of combined solar collector-geothermal heat pump systems to supply thermal load needed for heating greenhouses. *Energy Convers Manage* 2015;97:382–92.
- [14] Zhu N, Wang J, Liu L. Performance evaluation before and after solar seasonal storage coupled with ground source heat pump. *Energy Convers Manage* 2015;103:924–33.
- [15] Chargui R, Sammouda H. Modeling of a residential house coupled with a dual source heat pump using TRNSYS software. *Energy Convers Manage* 2014;81:384–9.
- [16] Wang G, Quan Z, Zhao Y, Sun C, Deng Y, Tong J. Experimental study on a novel PV/T air dual-heat-source composite heat pump hot water system. *Energy Build* 2015;108(1):175–84.
- [17] Tsai HL. Modeling and validation of refrigerant-based PVT-assisted heat pump water heating (PVTa-HPWH) system. *Sol Energy* 2016;122:36–47.
- [18] Good C, Andresen I, Hestnes AG. Solar energy for net zero energy buildings – a comparison between solar thermal, PV and photovoltaic-thermal (PV/T) systems. *Sol Energy* 2015;122:986–96.
- [19] Calise F, d'Accadia MD, Figaj RD, Vanoli L. A novel solar-assisted heat pump driven by photovoltaic/thermal collectors: dynamic simulation and thermoeconomic optimization. *Energy* 2016;95:346–66.
- [20] Good C, Chen J, Dai Y, Hestnes AG. Hybrid-photovoltaic thermal systems in buildings – a review. *Energy Proc* 2015;70:683–90.
- [21] Good C. Environmental impact assessments of hybrid photovoltaic-thermal (PV/T) systems – a review. *Renew Sustain Energy Rev* 2016;55:234–9.
- [22] Kuang YH, Wang RZ, Yu LQ. Experimental study on solar assisted heat pump system for heat supply. *Energy Convers Manage* 2003;44:1089–98.
- [23] Svard CD, Mitchell JW, Beckman WA. Design procedure and application of solar assisted series heat pump systems. *ASME* 1981;103:135–43.
- [24] Cai J, Ji J, Wang Y, Huang W. Numerical simulation and experimental validation of indirect expansion solar-assisted multi-functional heat pump. *Renew Energy* 2016;93:280–90.
- [25] Chaturvedi SK, Gagrani VD, Abdel-Salam TM. Solar-assisted heat pump – a sustainable system for low-temperature water heating applications. *Energy Convers Manage* 2014;77:550–7.
- [26] Omojaro P, Breitkopf C. Direct expansion solar assisted heat pumps: a review of applications and recent research. *Renew Sustain Energy Rev* 2013;22:33–45.
- [27] Çağlar A, Yamali C. Performance analysis of a solar-assisted heat pump with an evacuated tubular collector for domestic heating. *Energy Build* 2012;54:22–8.
- [28] Ochs F, Dermentzis G, Feist W. Minimization of the residual energy demand of multi-storey passive houses – energetic and economic analysis of solar thermal and PV in combination with a heat pump. *Energy Proc* 2014;48:1124–33.
- [29] Papakostas KT, Papadopoulos AM, Vlahakis IG. Optimisation of thermal protection in residential buildings using the variable base degree-days method. *Int J Sustain Energy* 2005;24(1):19–31.
- [30] Kalogirou SA. Use of TRNSYS for modelling and simulation of a hybrid PV-thermal solar system for Cyprus. *Renew Energy* 2001;23:247–60.
- [31] Klein SA. A Design Procedure for Solar Heating Systems. Ph.D. Thesis. Department of Chemical Engineering, University of Wisconsin-Madison; 1976.
- [32] Perez R, Stewart R, Seals R, Guertin T. The development and verification of the Perez diffuse radiation model. Sandia Report SAND88-7030. (Sandia National Laboratories, Albuquerque, New Mexico, 87185, USA) October, 1988.
- [33] Kalogirou S. Solar energy engineering. Boston: Academic Press; 2009.
- [34] Bellos E, Tzivanidis C, Antonopoulos KA. Exergetic, energetic and financial evaluation of a solar driven absorption cooling system with various collector types. *Appl Therm Eng* 2016;102:749–59.